Environ. Sci. Technol. **2008,** *42,* 3676–3682

Simulation of Air Quality Impacts from Prescribed Fires on an Urban Area

YONGTAO HU,*,† M. TALAT ODMAN,† MICHAEL E. CHANG,‡ WILLIAM JACKSON,§ SANGIL LEE,‡ ERIC S. EDGERTON,|| KARSTEN BAUMANN,|| AND ARMISTEAD G. RUSSELL†

School of Civil and Environmental Engineering, Georgia Institute of Technology, Atlanta, Georgia 30332, School of Earth and Atmospheric Sciences, Georgia Institute of Technology, Atlanta, Georgia 30332, USDA Forest Service, Asheville, North Carolina 28801, and Atmospheric Research and Analysis, Inc., Cary, North Carolina 27513

Received July 10, 2007. Revised manuscript received February 20, 2008. Accepted February 22, 2008.

On February 28, 2007, a severe smoke event caused by prescribed forest fires occurred in Atlanta, GA. Later smoke events in the southeastern metropolitan areas of the United States caused by the Georgia—Florida wild forest fires further magnified the significance of forest fire emissions and the benefits of being able to accurately predict such occurrences. By using preburning information, we utilize an operational forecasting system to simulate the potential air quality impacts from two large February 28th fires. Our "forecast" predicts that the scheduled prescribed fires would have resulted in over 1 million Atlanta residents being potentially exposed to fine particle matter ($PM_{2.5}$) levels of 35 μg m^{-3} or higher from 4 p.m. to midnight. The simulated peak 1 h $PM_{2.5}$ concentration is about 121 μg m^{-3}. Our study suggests that the current air quality forecasting technology can be a useful tool for helping the management of fire activities to protect public health. With postburning information, our "hindcast" predictions improved significantly on timing and location and slightly on peak values. "Hindcast" simulations also indicated that additional isoprenoid emissions from pine species temporarily triggered by the fire could induce rapid ozone and secondary organic aerosol formation during late winter. Results from this study suggest that fire induced biogenic volatile organic compounds emissions missing from current fire emissions estimate should be included in the future.

Introduction

On February 28, 2007, thick smoke hit the Atlanta, GA metropolitan area. Within a couple of hours between 4:00 and 6:00 p.m., monitored hourly concentration of fine particulate matter ($PM_{2.5}$) soared up to almost 150 μg m^{-3} at several sites. Ultimately the monitored 24 h concentration (midnight to midnight) of $PM_{2.5}$ in Atlanta, 37.8 μg m^{-3}, exceeded the current National Ambient Air Quality Standard (NAAQS) of 35 μg m^{-3} (*1*). At the same time, hourly ozone (O_3) concentrations jumped by up to 30 ppb. Two prescribed fires in adjacent wildlands about 80 km southeast of Atlanta, one in the Oconee National Forest (Oconee NF) and the other in the Piedmont National Wildlife Refuge (Piedmont NWR) (called Fire O and P hereafter, Figure 1a), together totaling about 12 km^2, were blamed for "smoking out" metropolitan Atlanta at the time "commuters headed home and ball teams took to the fields" (*2*). On the same day there were numerous other smaller fires state-wide recorded by the Georgia Forestry Commission (Figure 1a). As reported in the popular press, asthma attacks, apparently triggered by the smoke or ozone, were reported by asthmatics that were able to self-medicate, as well as pediatric clinics that were receiving pulmonary patients the next day (*2*). Impacts on more severe responses have not yet been quantified.

Fire has been a management tool in the United States used to sustain healthy wildland ecosystems and to reduce the risk of catastrophic wildfires. For example, the two burns were designed to reduce hazardous fuels and enhance the southern pine habitat for the endangered red-cockaded woodpeckers (*Picoides borealis*) (*2*). Nationwide about 10 000 km^2 lands were burn-treated in 2006 (http://www.nifc.gov/stats/prescribed_fires.html). However, burning of wildland vegetation increases the emissions of air pollutants such as $PM_{2.5}$, carbon monoxide (CO), volatile organic compounds (VOC), and nitrogen oxides (NO_x), which impact air quality, visibility and potentially public health. To protect public health and welfare, the U.S. Environmental Protection Agency (U.S. EPA) recommends that land managers and state/local/tribal air quality managers work together to coordinate fire activities especially at the wildland/urban interface to minimize air pollution impacts (*3*). Of interest is to what degree impacts of fires can be forecast to help plan and conduct burns.

The question for the scientific community is "with our current knowledge and technology, how predictable is a smoke event like the one on February 28 so that the burn could be postponed and conducted under different meteorological conditions, or changes made (such as reducing the size of the fires) to release less emissions into the atmosphere?" There are several air quality forecasting systems currently operational in the United States at either national (e.g., NOAA/EPA's Eta-CMAQ system covering eastern U.S. with 12 km resolution *4, 5*) or regional levels covering one or more particular metropolitan areas (e.g., MM5-CMAQ system serving Houston and Dallas, Texas (*6*), and UAM (*7*) and WRF-CMAQ systems serving Atlanta, Georgia (*8*),). These tools have enjoyed reasonable forecasting accuracy over the past years (*5*). Fire emissions' impacts are included in these air quality forecasts but only as averages of historical fire events to represent typical fire emissions on any given day, in essence smoothing individual, more intense events both spatially and temporally.

Recent experiments measuring emission factors of biomass fires predominantly relying on laboratory scale experiments have provide updated emissions factors (*9–15*). Combining these factors with information on fuel type and loading, burn size, location, and timing obtained from either fire count records or satellite retrievals, one can estimate fire emissions from individual and regional biomass burning (*16, 17*). Fire emissions for the Southeastern U.S. were recently updated in this manner (*18*). Satellite detected active fire data have

* Corresponding author phone: 404-894-1854; fax: 404-894-8266; e-mail: yh29@mail.gatech.edu.
† School of Civil and Environmental Engineering, Georgia Institute of Technology.
‡ School of Earth and Atmospheric Sciences, Georgia Institute of Technology.
§ USDA Forest Service.
|| Atmospheric Research and Analysis, Inc.

10.1021/es071703k CCC: $40.75
Published on Web 04/11/2008

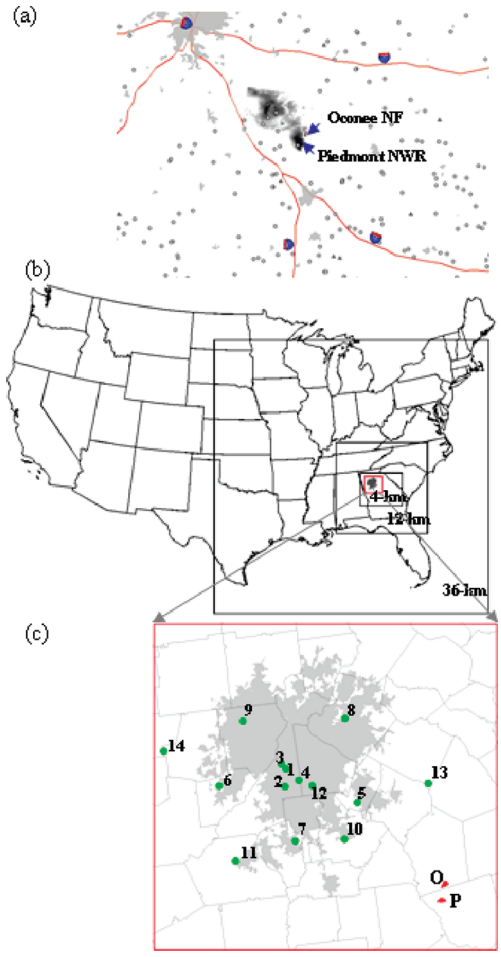

FIGURE 1. (a) Smoke detected near the Atlanta metropolitan area at 1:15 and 1:45 p.m. Eastern Standard Time (EST) on February 28, 2007 by using the Geostationary Satellite (GOES) data (received from National Oceanic and Atmospheric Administration). After 1:45 p.m. the high clouds prevented seeing any further spread of the smoke with the GOES images. The smoke seen on the GOES images originated from the prescribed fires within the Oconee NF and Piedmont NWR. The circles represent other burned areas between 0.007 and 0.47 km^2 while the triangles represent those between 0.47 and 1.11 km (*2*), according to data recorded by the Georgia Forestry Commission. Urban areas are in light gray. (b) Atlanta metropolitan area is shown in light gray on a U.S. map along the Hi-Res modeling domains, with the 36, 12, and 4 km horizontal grid resolutions, respectively. (c) Air quality monitoring sites Jefferson Street^{*,a,b} (1), Fort McPherson^{*,a} (2), Fire Station 8^{*,a} (3), Confederate Ave^{*,a,b} (4), Conyers^{b} (5), Douglasville^{b} (6), Fayetteville^{*,b} (7), Gwinnett^{*,a,b} (8), Kennesaw^{*,b} (9), McDonough^{a,b} (10), Newnan^{a,b} (11), South Dekalb^{*,a,b} (12), Walton^{a} (13), and Yorkville^{a,b} (14) are shown as green dots on a map with the Atlanta urban area shown in light gray. The sites with a* are considered Atlanta urban sites, those with an^{a} are $PM_{2.5}$ sites and with a^{b} are O_3 sites. Also shown in red are the actual burned areas of Fires O and P.

also been utilized to refine the U.S. national fire emission inventory for major wildfire events (*19*). These inventories, along with air quality models, are used to investigate fire plume evolution (*20, 21*) and smoke impacts on air quality from wild and prescribed forest fires (*22, 23*). However a comprehensive forecast of such smoke impacts is still in its initial stages (*24*).

Here we utilize an existing advanced regional air quality forecasting system, currently serving the Atlanta metropolitan area at a 4 km resolution, to simulate the February 28th smoke event. This operational system forecasts primary and secondary air pollutant concentrations one day in advance. As such, it would allow land managers choose to wait for more favorable meteorological conditions and allow air quality managers to take the burns into consideration when predicting the Air Quality Index (AQI) for the next day. Here, the model is first exercised in the forecast mode using forecast meteorological fields and burning plans. Next, to assess how much additional knowledge can improve the results, a set of hindcasts are conducted, utilizing reanalysis fields, observed meteorology for data assimilation, and information on actual fire evolution.

Materials and Methods

We use Hi-Res, a regional forecasting system which provides local air quality forecasts for the metropolitan Atlanta area since 2006 (*8*), to predict the air quality impacts from the February 28th prescribed fires set in central Georgia's federal wildlands. Hi-Res (Figure S1a, Supporting Information) uses the Weather Research and Forecasting model (WRF, version 2.2) for forecasting meteorology (wrf-model.org), the Sparse Matrix Operator Kernel Emissions model (SMOKE, version 2.1) for gridded emissions (*25*), and the Community Multiscale Air Quality model (CMAQ, version 4.6) for chemistry and transport (*26*) updated with strict mass conservation (*27*) and equipped with the SAPRC-99 chemical mechanism (*28*). The emissions inventory used in Hi-Res as input to SMOKE is projected from a 2002 "typical year" inventory (*18*). Hi-Res nests its 4 km forecasting grid in a 12 km mother grid covering Georgia and portions of neighboring states and uses a 36 km outer grid over the eastern U.S. to provide air quality boundary conditions (Figure 1b). Hi-Res first simulates a 77 h (3 days plus 5 h) period starting from 00Z on the 36 km grid. WRF is initialized and constrained at the boundaries using 00Z 84 h forecast products from the North American Mesoscale (NAM) model (nomads.ncdc.noaa.gov), and CMAQ is initialized from the previous forecasting cycle and uses "clean" boundary conditions (Figure S1b, Supporting Information). Then Hi-Res simulates the same 77 h period on the 12 km grid and nests down to the 4 km grid for the last 32 h. WRF is initialized and constrained at the boundaries using 00Z NAM forecasts, while CMAQ is initialized from the previous forecasting cycle and uses the 36 km forecasts for air quality boundary conditions. The simulations take about 12 h on six dedicated CPUs.

To "forecast" air quality impacts from the two February 28th prescribed fires O and P, we estimated their emissions using information collected from the prescribed fire plans prepared in advance by the technical staff on the Oconee NF and Piedmont NWR. Preburning information includes the acreage of the planned burning area, approximate locations, fuel load descriptions, and operation schedules. Since there is a lack of information for precisely separating flaming and smoldering stages during the estimation of emissions, we chose composite emission factors (Table S1, Supporting Information) and estimated hourly fuel consumptions that merge the two stages together (*18*). We calculated emissions for each pollutant in Table S1 and allocated them to the 12 and 4 km grid cells according to the approximate fire locations. Vertical distribution of fire emissions are based on the assumption of a 1 km plume rise during a fair weather day in late winter. Gridded emissions of fires O and P were added to other emissions for the Hi-Res standard forecast. We first ran Hi-Res starting from February 26th 00Z through March first 05Z at its standard configuration with "typical" emissions, then reran Hi-Res' CMAQ only for the last 32 h on the 12 and 4 km grids with the emissions from fires O and P added in. The difference between simulated air quality fields from the above two Hi-Res runs is the contribution of emissions from fires O and P. To evaluate this fire-impact

"forecast", air quality fields simulated with "fire emissions" were compared with hourly air quality observations, mainly for O_3, $PM_{2.5}$, and elemental/black carbon (EC), collected at monitoring sites located in the Atlanta metropolitan area (Figure 1c). Multiple sites captured the dramatic jumps of both O_3 and $PM_{2.5}$ during the smoke event (*29*). Among them, only the SouthEastern Aerosol Research and CHaracterization (SEARCH) (*30*) site at Jefferson Street (JST) measured hourly concentrations of $PM_{2.5}$ components such as nitrate, sulfate, ammonium, EC, and total carbon in addition to O_3 and $PM_{2.5}$ mass.

As an extension to the "forecast" of air quality impacts, the total population of potential exposures caused by the specific fires was calculated by adding up the population (Census 2000, www.census.gov) living in the grid cells that receives "fire emissions" contributions and have a predicted $PM_{2.5}$ concentration higher than 35μg m^{-3} (the current 24 h NAAQS) or 65μg m^{-3} (the prior NAAQS). Here the population of potential exposures is based on static residential statistics as an approximation to the actual population in the area covered by a grid cell (16 km^2) as population activity is not considered. Such "fire impact" information can be useful for land managers to interpret the simulated concentrations and ultimately help them to make to-burn-or-not-to-burn decisions.

To further assess the predictive capability of Hi-Res on specific fire-impacts and identify key weaknesses we also conducted a set of hindcasts of this Atlanta smoke event. First, the emissions from Fires O and P were re-estimated by using the Fire Emission Production Simulator (FEPS) (*31*) with extra information collected and prepared after the burns (Table S2, Supporting Information). Postburning information includes the actual acreage burned each hour with fuel moisture information and fuel consumption estimated using the Consume 3.0 model (http://www.fs.fed.us/pnw/fera/research/smoke/consume/index.shtml) and hourly flaming/smoldering stage information, plus local meteorology and fire temperature information for estimating hourly plume rise. Hourly "fire emissions" were then allocated horizontally into the 12 and 4 km grid cells according to the actual burned area in the cell and distributed vertically using hourly plume rise information. As in the "forecast", we also ran Hi-Res for this hindcast (called HINDEMIS hereafter) twice, once with "typical" emissions and a second time with the "actual" emissions from fires O and P added. Note that HINDEMIS keeps the meteorological fields the same as those used for the "forecast". Then, keeping the "actual" emissions, we replaced the meteorology with hindcast fields and conducted a second hindcast (HINDMET): this time, reanalysis products from NAM were utilized to initialize WRF, constrain boundary conditions and nudge simulated fields at 6 h intervals (*32*). Finally, we conducted the final hindcast (called "hindcast" hereafter) with increased biogenic VOC emissions from trees due to exposure to fires O and P and the elevated temperatures (*33*) using hindcast meteorological fields and the "actual" emissions. Due to lack of information at this moment, we are unable to conduct a full hindcast in which the "typical" emissions should be fully updated with actual emissions such as from power plants reports, biomass fires records, and etc.

Results and Discussion

Our "forecast" simulated that Fires O and P together significantly impacted the air quality of Atlanta on February 28th 2007 from late afternoon to midnight (Figure 2a). The "fire impact" reached its maximum between 10:00 and 11:00 p.m., when over 1 million Atlantans were estimated to have potential 1 h exposures of 35 μg m^{-3} or higher $PM_{2.5}$ concentrations, with 670 000 of them potentially exposed to over 65 μg m^{-3} or more. Our "forecast" predicted that 380 000 Atlantans had potential 24 h exposures to 35 μg m^{-3} or higher $PM_{2.5}$ concentrations on February 28th, 2007 and none to over 65 μg m^{-3}. The maximum predicted increase was 94 μg m^{-3} in the Atlanta urban area (defined as having a population density higher than 5000 per square mile (www.census.gov)), driving up ambient $PM_{2.5}$ concentrations to a peak of 121 μg m^{-3} between 8:00 and 9:00 p.m. (Figure 2b), while the highest observed 1 h concentration was 149 μg m^{-3}. The simulated maximum 24 h $PM_{2.5}$ concentration in Atlanta urban area was 47.5 μg m^{-3} compared to the observed 37.8 μg m^{-3}.

Comparing the "forecasts" with the hourly $PM_{2.5}$ measurements, i.e. the predicted maximum within the Atlanta urban area versus the observed maximum among the Atlanta urban sites, there is good agreement after 8:00 p.m. but the predictions are low by 50 μg m^{-3} or more for the late afternoon hours (Figure 2b) when the observations peaked. On the other hand, comparison of "forecast" with observed EC at JST shows very similar levels in the late afternoon hours, and an overestimation after 9:00 p.m. (Figure 3a). The EC performance at JST suggests that the primary emissions from fires O and P, including organic carbon (OC), were not underestimated significantly as seen in $PM_{2.5}$ total mass. However, the difference of hourly ratios of fine organic matter (OM) to total $PM_{2.5}$, "forecast" mean vs observed at JST (Figure 3b), suggests that there is substantial OM missing from the predicted $PM_{2.5}$ concentrations, especially during the early hours of the smoke event. To convert OC observed at JST to OM, a factor of 1.2, representing urban emissions, was used before the smoke hit Atlanta and a factor of 1.6, representing OM dominated by burning, was used afterward (*34–36*). Combination of above findings indicates a possible significant underestimation of secondary organic aerosol (SOA) in our "forecast".

Along with an under-prediction in $PM_{2.5}$, the increase in O_3 coinciding with the "fire impact" is significantly underestimated. The "forecast" peak O_3 contribution of fires O and P is less than 8 ppb, while observations increased by up to 30 ppb (Figure 2c). This indicates a lack of simulated photochemical production and suggests a possible lack of precursors emitted from the burning. A second possibility is enhanced photolytic forcing in the plume, though given the absorption of smoke, this is unlikely. Our sensitivity tests showed that O_3 contribution of fires O and P is relatively insensitive to their NO_x emissions, but increases in proportion to adding their VOC emissions. These results support that VOC precursors were possibly underestimated consistent with possible insufficient SOA formation. The short time available from the time of emission to impacting Atlanta (2∼3 h) further suggests that very reactive VOCs were involved.

While pine is the dominant tree species in the burned area, the target of both prescribed fires was actually the forest floor, which typically is dominated by needle litter, bark rot, twigs, duff, wiregrass, and shrubs (http://depts.washington.edu/nwfire/dps/). Nevertheless, pine trees in the area were exposed to either the fire directly or the elevated-temperature caused by the fire. Laboratory experiments have shown that exposure of pines to fire and to the associated elevated temperature may induce bursts of isoprenoid (isoprene and monoterpenes) emissions temporarily during and after fire treatment (*33*). In situ measurements have also indicated that emissions (in g-species/kg-biomass) from the smoldering stage are generally higher than those from flaming and also higher than reported for laboratory burnings, especially for aromatic and biogenic compounds such as benzene, toluene, xylenes, isoprene, and pinenes, which at least in part can be attributed as indirectly emitted by the heat-exposed vegetation instead of being a direct combustion product (*15*). This category of extra biogenic VOC emissions that is not emitted from the fuel loads but induced by the fire is ignored from the previous fire emissions estimates and traditional emissions estimates. Note that both isoprene and monoterpenes are very reactive VOCs and precursors of

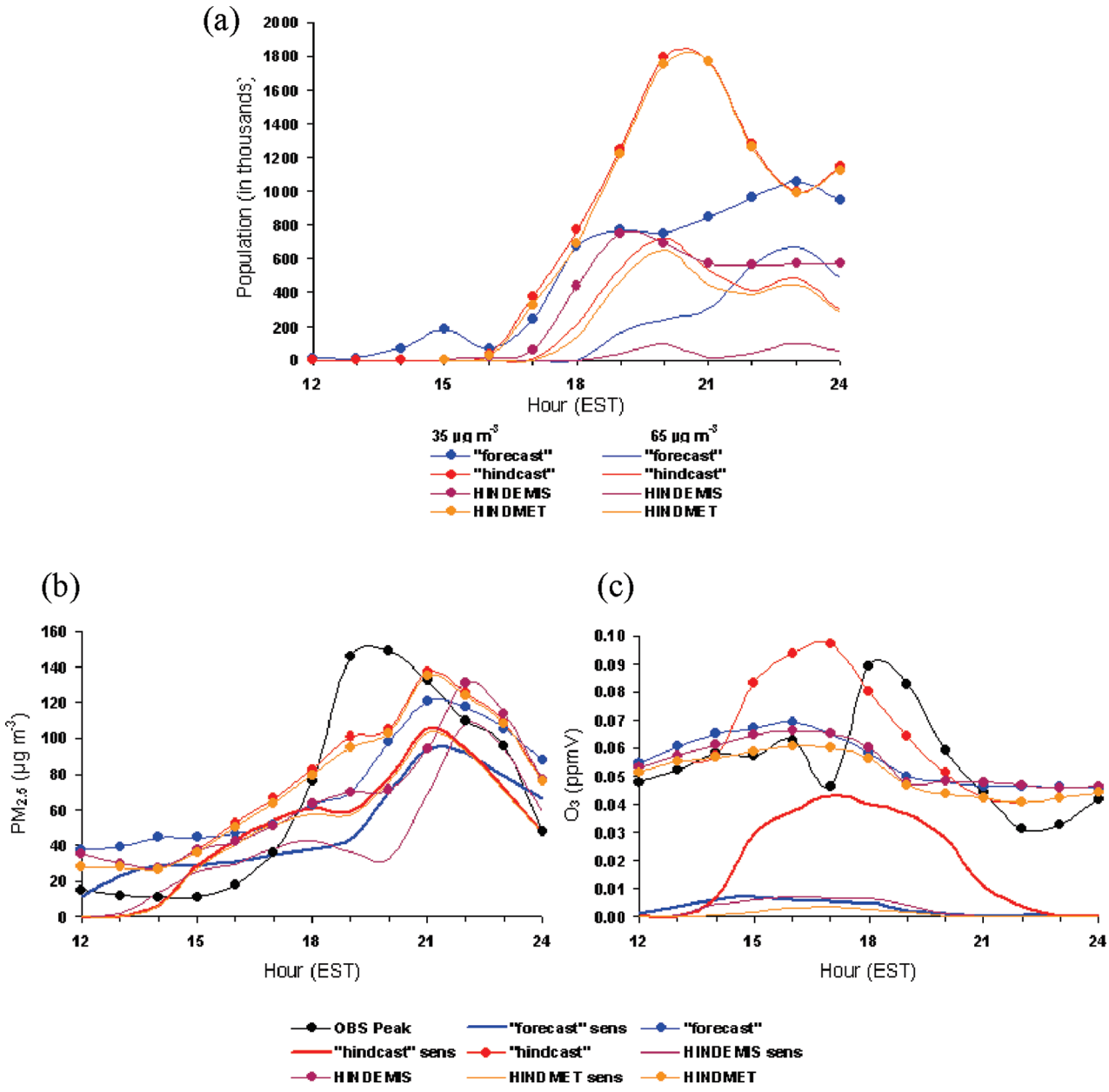

FIGURE 2. Simulation results: (a) Predicted hourly total Atlanta urban population exposed to 35 μg m^{-3} and 65 μg m^{-3} or higher ambient $PM_{2.5}$ concentration; (b) Predicted maximum ambient $PM_{2.5}$ concentration within the Atlanta urban area and predicted maximum contributions of fires O and P (labeled with "sens" in the legend) to $PM_{2.5}$, versus the observed $PM_{2.5}$ maximum among the Atlanta urban sites; (c) Predicted maximum ambient O_3 concentration within the Atlanta urban area and predicted maximum contributions of fires O and P to O_3 versus the observed O_3 maximum among the Atlanta urban sites. Note that hour 18 on the *x*-axis represents the hour between 5:00 and 6:00 p.m. EST.

SOA (*37*, *38*). This is also supported by observations of elevated ambient concentrations of secondary organic tracers during the event (*39*). We conducted sensitivity tests with extra biogenic VOC emissions in "forecast" for fires O and P to assess how much additional VOC might be added. An increase of four times the amount of "forecast" VOC emissions is suggested by the sensitivity testing results and is adopted in "hindcast".

By adding, step by step, a better emissions estimate, a better meteorology, and the enhanced biogenic VOC emissions, we investigated how much each of them affects our fire impact predictions. The HINDEMIS, with "actual" emissions, improves little of the underestimation of maximum $PM_{2.5}$ concentrations during hours between 6:00 and 9:00 p.m. (Figure 2b), though it predicts a higher peak $PM_{2.5}$ concentration as 131 μg m^{-3}, which is closer to the observation (Table 1). The more accurate locations of emissions modified little the simulated path of the plume (not shown). But apparently the change in the profile of hourly emission rates (Figure S2, Supporting Information) helps to predict a better timing of maximum "fire impacts". HINDEMIS predicts a peak "fire impact" between 6:00 and 7:00 p.m. (Figure 2a) corresponding to the earlier decline of emission rates, whereas observed $PM_{2.5}$ at most of the sites impacted by the smoke peaked around that hour and the hour after.

HINDMET, on the other hand, improves the prediction of plume path because of the better meteorology. The spatial distribution of the "forecast" and the "hindcast" $PM_{2.5}$ plumes (HINDMET and "hindcast" simulated similar plume paths) along with peak observations, which suggest a spatial extent for the observed plume, are shown in Figure 4. We calculated that there is about a 20 degree prediction error of the $PM_{2.5}$ plume direction in the "forecast", whereas a 10 degree error remains in the "hindcast"/HINDMET. This suggests that reanalysis data utilized with nudging technology improved

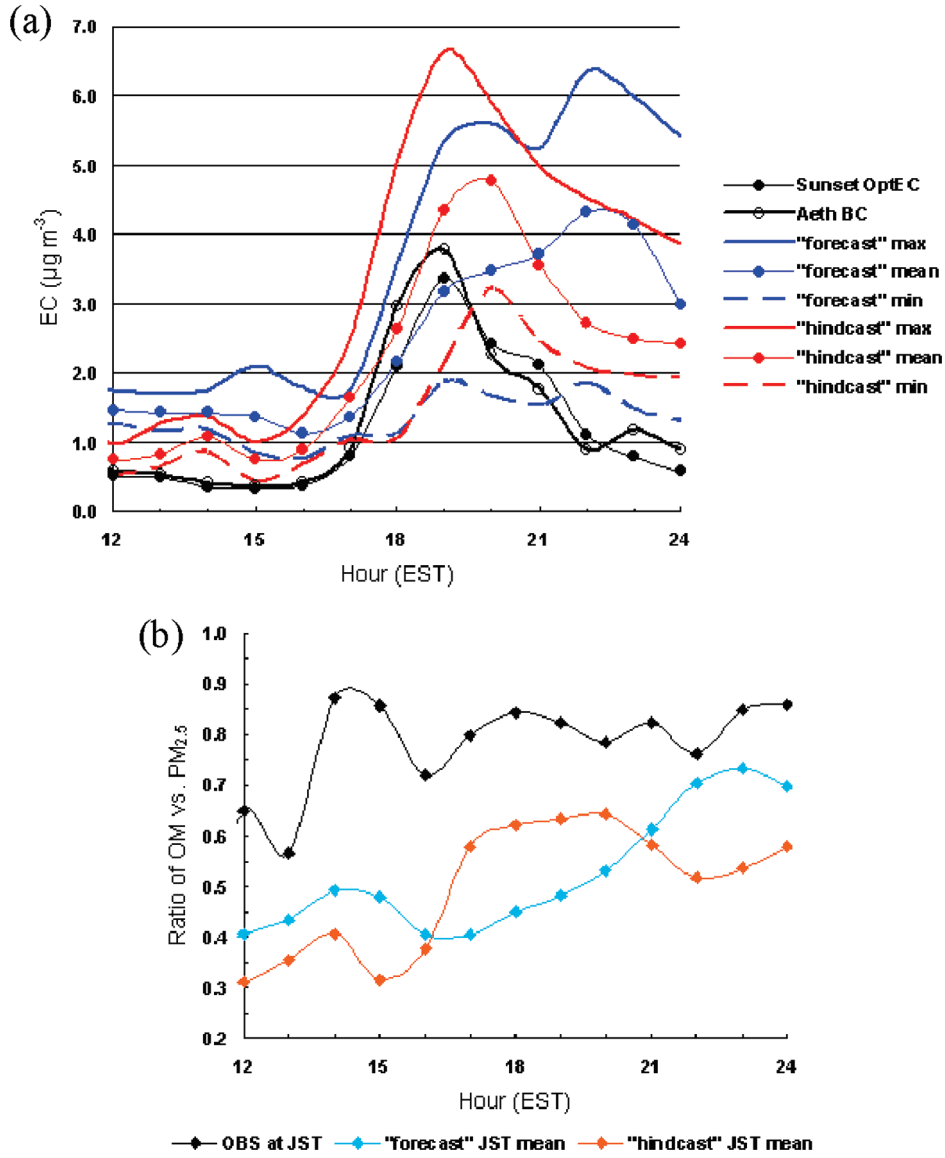

FIGURE 3. (a) Predicted hourly maximum, mean and minimum EC concentrations at JST versus the observed using EC Sunset (Sunset OptEC) and BC Aethalometer (Aeth BC); Maximum, mean and minimum values are taken from areas within the 5 × 5 block of grid cells around JST; (b) Hourly ratios of OM to total $PM_{2.5}$, predicted mean at JST versus the observed.

TABLE 1. Observed and Simulated Peak Values

	observation	"forecast"	HINDEMIS	HINDMET	"hindcast"
peak ozone (ppb)	89	69	66	61	97
time of peak ozone (EST hour)	18	16	16	16	17
peak $PM_{2.5}$ (μg m^{-3})	149	121	131	135	137
time of peak $PM_{2.5}$ (EST hour)	20	21	22	21	21
peak impacts[a] (population in thousands)	n/a	1056	752	1768	1789
time of peak impacts (EST hour)	n/a	23	19	21	20

[a] Represented using total population that having potential 1 h exposures of 35 μg m^{-3} or higher $PM_{2.5}$ concentrations.

simulated surface wind fields, though to a limited degree. However, the limited modification of simulated plume path changed the distribution of maximum $PM_{2.5}$ concentrations and significantly improved the predictions of $PM_{2.5}$ concentrations during hours between 5:00 and 9:00 p.m. (Figure 2b). Because of the modified plume path in HINDMET passing over populated area in a much higher density, the prediction of "fire impacts" doubled in population of potential exposures (Figure 2a). The peak $PM_{2.5}$ prediction in HINDMET was also improved to 135 μg m^{-3}, with a better timing (Table 1).

However, both the better emissions estimate and better meteorology changed O_3 predictions very little. In contrast to other simulations, "hindcast" results, with the enhanced biogenic emissions, capture the observed O_3 increases relatively well (Figure 2c). The "hindcast" predicts a maximum jump in O_3 concentration of 40 ppb due to the extra biogenic VOC emissions. Note that the drop in observed maximum O_3 between 4:00 and 5:00 p.m. is due to lack of data at a number of monitoring sites. The "hindcast" also improves $PM_{2.5}$ predictions by adding extra SOA on top of the

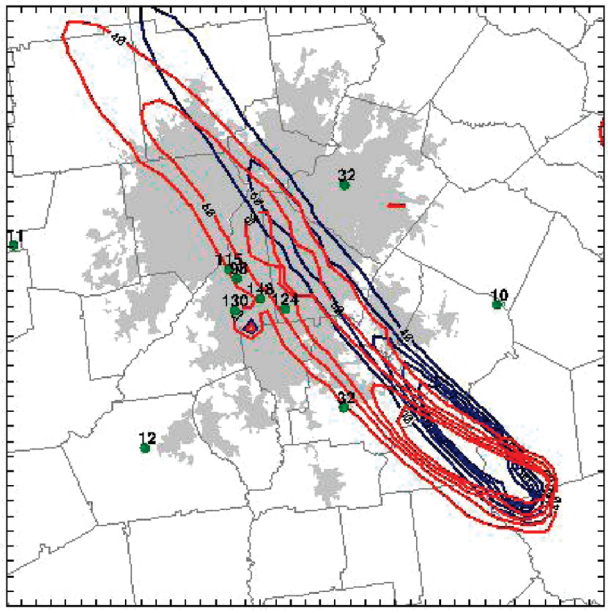

FIGURE 4. Spatial distribution of "forecast" (blue) and hindcast (red) plumes, shown as contours of $PM_{2.5}$ concentrations at 20 $\mu g\ m^{-3}$ intervals (starting at 40 $\mu g\ m^{-3}$ and ending at 120 $\mu g\ m^{-3}$) between 7:00 and 8:00 p.m., along with observed plume suggested by the measured values (in $\mu g\ m^{-3}$) shown above the site locations (green dots).

HINDMET $PM_{2.5}$ concentrations, though the enhancement of SOA formation due to increased biogenic VOC emissions is limited with the largest less than 5 $\mu g\ m^{-3}$ (Figure 2b). It is suggested by this study that the enhanced biogenic VOC emissions from trees due to exposure to fire and its elevated temperatures should be included in future simulations of fire-caused photochemical smoke events, and current inventories should be corrected for these fire effects.

Our "hindcast" simulated more Atlantans would be potentially impacted by the fires (Figure 2a). The "fire impact" reached its maximum between 7:00 and 8:00 p.m., when population of potential 1 h exposure to $PM_{2.5}$ levels greater than 35 and 65 $\mu g\ m^{-3}$ would increase to 1.8 million and 720 000, respectively (Figure 2a). This predicted peaking time (three hours earlier than the "forecast" prediction) is consistent with the peak $PM_{2.5}$ observations (Table 1). The hourly burning information collected after the fire significantly improves timing. This better hourly profile of emission rates also improves EC performance of "hindcast" at JST: now no underestimation is seen during the beginning hours of the smoke event and the overestimation after 9:00 p.m. decreased significantly (Figure 3a). With the $PM_{2.5}$ plume better simulated (Figure 4) and OM increased from both primary and secondary routes (Figure 3b), the simulated $PM_{2.5}$ exceeds 100 $\mu g\ m^{-3}$ between 6:00 and 7:00 p.m., compared to around 70 $\mu g\ m^{-3}$ from the "forecast" at that time (Figure 2b). Note that the "hindcast" reproduces the "forecast" $PM_{2.5}$ peaking time between 8:00 and 9:00 p.m., 1 h later than the measurements, but predicts the peak value at 137 $\mu g\ m^{-3}$ compared to 121 $\mu g\ m^{-3}$. The "hindcast" estimates 70 000 Atlantans were potentially exposed to 24 h $PM_{2.5}$ concentrations over 35 $\mu g\ m^{-3}$ and none to over 65 $\mu g\ m^{-3}$, with the maximum 24 h $PM_{2.5}$ concentration in Atlanta urban area of 55.8 $\mu g\ m^{-3}$.

With the increase of primary OM (as EC increases in Figure 3a) as well as extra SOA formed, "hindcast" $OM/PM_{2.5}$ ratios at JST show improvement over "forecast" during the hours of smoke impact (Figure 3b). However, they are still low compared to observations. As noted earlier, elevated $OM/PM_{2.5}$ ratios were observed even before the smoke hit (hour 17) and "hindcast" EC is overestimated during the same period (Figure 3). This suggests that in the "typical" emissions used in this study, some sources with higher OC/EC ratios such as open fires are either missing or underestimated, whereas others with higher EC/OC ratios such as diesel engines are overestimated. For example, on February 28, 2007, emissions from open burnings, i.e., wildfires and permitted prescribed burnings, was larger than a "typical" year in the southeastern U.S. Using preliminary Georgia Forestry Commission data we estimated that there were about 1.1×10^9 g $PM_{2.5}$ emissions from open fires in Georgia excluding O and P, whereas the total "typical" fire emissions in Georgia's inventory accounted for only 0.5×10^9 g (Figure S3, Supporting Information). Missing open fires would contribute to the regional "background" via both direct OM emissions and SOA formation.

Another reason for the lower $OM/PM_{2.5}$ ratios is systematically low SOA formation in CMAQ predictions. We calculated that at JST the CMAQ predicted SOA/OM ratio is around 20% on average, while it is only 13% during the hours between 6:00 and 9:00 p.m. when smoke hit JST. However, using a measurement-based method, this ratio was estimated as 44% during the event (*39*). Recent studies suggest that the current SOA module in CMAQ, as well as those in other photochemical models, tends to underestimate SOA production (*40–43*). The actual SOA enhancement could be much higher leading to a higher OM prediction if new processes such as oligimerization and polymerization, which have been identified as significant sources of SOA (*44–47*), were included. This might close the gap between "hindcast" $PM_{2.5}$ predictions and observations during the hours between 6:00 and 8:00 p.m. (Figure 2b).

Acknowledgments

This work was funded in part by U.S. Environmental Protection Agency under grants R-82897601, RD83096001, and RD83107601, as well as NASA, and Georgia Power. The forecasting operation is sponsored by the Georgia Department of Natural Resources under contract no. 775-790159. We thank Tom Atkinson of Georgia EPD for providing burning plan information. We also extend our gratitude to Axel Graumann and Mike Squires of NOAA for providing the Polar satellite imagery.

Supporting Information Available

Figures presenting components of Hi-Res system and Hi-Res forecasting cycle, plot of hourly $PM_{2.5}$ emission rates of fires O and P, plot showing spatial distribution of "typical" fire emissions, and tables presenting emission factors and emissions summary of fires O and P. This material is available free of charge via the Internet at http://pubs.acs.org.

Literature Cited

(1) U.S. EPA. National Ambient Air Quality Standards for Particulate Matter; Final Rule. Environmental Protection Agency *Code of Federal Regulations*, 40 CFR Part 50, **2006**.

(2) Shelton, S. Smoke Slipped up on Experts. The Atlanta Journal-Constitution, 03/02/07, Atlanta, Georgia, 2007; http://www.ajc.com/search/content/metro/stories/2007/03/01/0302meshsmoke.html.

(3) Air Quality Policy on Wildland and Prescribed Fires (Interim Report); U. S. Environmental Protection Agency, 1998.

(4) Otte, T.; Pouliot, G.; Pleim, J.; Young, J.; Schere, K.; Wong, D.; Lee, P.; Tsidulko, M.; McQueen, J.; Davidson, P.; Mathur, R.; Chuang, H.; Dimego, G.; Seaman, N. Linking the Eta model with the community multiscale air quality (CMAQ) modeling system to build a national air quality system. *Weather Forecast* **2005**, *20*, 367–384.

(5) Eder, B.; Kang, D.; Mathur, R.; Yu, S.; Schere, K. An operational evaluation of the Eta-CMAQ air quality forecast model. *Atmos. Environ.* **2006**, *40*, 4894–4905.

(6) Byun, D. W.; Jang, M.-D.; Kim, S. T.; Perma, R. Development and Operational Evaluation of the Eastern Texas Air Quality (ETAQ) Forecasting System. *4th Annual CMAS Models-3 Users' Conference* Friday Center, UNC-Chapel Hill, 2005.

(7) Chang, M. E.; Cardelino, C. Application of the urban airshed model to forecasting next-day peak ozone concentration in Atlanta, Georgia. *J. Air Waste Manage. Assoc.* **2000**, *50*, 2010–2024.
(8) Odman, M. T.; Hu, Y.; Chang, M. E.; Russell, A. G. Forecasting ozone and $PM_{2.5}$ in southeastern U.S. In *Developments in Environmental Science*; Borrego, C., Renner, E., Eds.; Elsevier Ltd.: New York, 2007; Vol *6*, pp 219−288.
(9) Ward, D. E.; Hardy, C. C. Smoke emissions from wildland fires. *Environ. Inte.* **1991**, *17*, 117–134.
(10) Yokelson, R. J.; Griffith, D. W. T.; Ward, D. E. Open-path Fourier transform infrared studies of large-scale laboratory biomass fires. *J. Geophys. Res.* **1996**, *101* (D15), 21067–21080.
(11) Yokelson, R. J.; Susott, R.; Ward, D. E.; Reardon, J.; Griffith, D. W. T. Emissions from smoldering combustion of biomass measured by open-path Fourier transform infrared spectroscopy. *J. Geophys. Res.* **1997**, *102* (D15), 18,865–18,877.
(12) Yokelson, R. J.; Goode, J. G.; Ward, D. E.; Susott, R. A.; Babbitt, R. E.; Wade, D. W.; Bertschi, I.; Griffith, D. W. T.; Hao, W. M. Emissions of formaldehyde, acetic acid, methanol, and other trace gases from biomass fires in North Carolina measured by airborne Fourier transform infrared spectroscopy. *J. Geophys. Res.* **1999**, *104* (D23), 30,109–30,125.
(13) Bertschi, I.; Yokelson, R. J.; Ward, D. E.; Babbitt, R. E.; Susott, R. A.; Goode, J. G.; Hao, W. M. Trace gas and particle emissions from fires in large diameter and belowground biomass fuels *J. Geophys. Res.* **2003***108*D138472, doi: 10.1029/2002JD002100.
(14) Sinha, P.; Hobbs, P. V.; Yokelson, R. J.; Blake, D. R.; Gao, S.; Kirchstetter, T. W. Emissions from miombo woodland and dambo grassland savanna fires *J. Geophys. Res.* **2004***109*D11305, doi:doi:10.1029/2004JD004521.
(15) Lee, S.; Baumann, K.; Schauer, J. J.; Sheesley, R. J.; Naeher, L. P.; Meinardi, S.; Blake, D. R.; Edgerton, E. S.; Russell, A. G.; Clements, M. Gaseous and particulate emissions from prescribed burning in Georgia. *Environ. Sci. Technol.* **2005**, *39*, 9049–9056.
(16) Clinton, N. E.; Gong, P.; Scott, K. Quantification of pollutants emitted from very large wildland fires in southern California, USA. *Atmos. Environ.* **2006**, *40*, 3686–3695.
(17) Wiedinmyer, C.; Quayle, B.; Geron, C.; Belote, A.; McKenzie, D.; Zhang, X.; O'Neill, S.; Wynne, K. K. Estimating emissions from fires in North America for air quality modeling. *Atmos. Environ.* **2006**, *40*, 3419–3432.
(18) MACTEC. Documentation of the Revised 2002 Base Year, Revised 2018, and Initial 2009 Emission Inventories for VISTAS; Visibility Improvement State and Tribal Association of the Southeast (VISTAS): Forest Park, GA, 2005.
(19) Roy, B.; Pouliot, G. A.; Gilliland, A.; Pierce, T.; Howard, S.; Bhave, P. V.; Benjey, W. Refining fire emisisons for air quality modeling with remotely sensed fire counts: A wildfire case study. *Atmos. Environ.* **2007**, *41*, 655–665.
(20) Mason, S. A.; Trentmann, J.; Winterrath, T.; Yokelson, R. J.; Christian, T. J.; Carlson, L. J.; Warner, T. R. Intercomparison of two box models of the chemiscal evolution in biomass-burning smoke plumes. *J. Atmos. Chem.* **2006**, *55*, 273–297.
(21) Saarikoski, S.; Sillanpää, M.; Sofiev, M.; Timonen, H.; Saarnio, K.; Teinilä, K.; Karppinen, A.; Kukkonen, K.; Hillamo, R. Chemical composition of aerosols during a major biomass burning episode over northern Europe in spring 2006: Experimental and modeling assessments. *Atmos. Environ.* **2007**, *41*, 3577–3589.
(22) Tian, D.; Wang, Y.; Bergin, M.; Hu, Y.; Liu, Y.; Russell, A. G. Air quality impacts from prescribed forest fires under different management practices *Environ. Sci. Technol.* **2007** [Online early access]. DOI: 10.1021/es0711213 . Published online: March 5, **2008**.
(23) Junquera, V.; Russell, M. M.; Vizuete, W.; Kimura, Y.; Allen, D. Wildfires in eastern Texas in August and September 2000: Emissions, aircraft measurements, and impact on photochemistry. *Atmos. Environ.* **2005**, *39*, 4983–4996.
(24) McKenzie, D.; O'Neill, S. M.; Larkin, N. K.; Norheim, R. A. Integrating models to predict regional haze from wildland fire. *Ecol. Model.* **2006**, *199*, 278–288.
(25) CEP. *Sparse Matrix Operator Kernel Emissions Modeling System (SMOKE) User Manual*; Carolina Environmental Program—The University of North Carolina at Chapel Hill: Chapel Hill, NC, 2003.
(26) Byun, D. W.; Ching, J. K. S. *Science algorithms of the EPA Models-3 Community Multiscale Air Quality (CMAQ) Modeling System*, EPA/600/R-99/030; Environmental Protection Agency: Washington, DC, 1999.
(27) Hu, Y.; Odman, M. T.; Russell, A. G. Mass conservation in the Community Multiscale Air Quality model. *Atmos. Environ.* **2006**, *40*, 1199–1204.
(28) Carter, W. P. L. *Documentation of the SAPRC-99 Chemical Mechanism for VOC Reactivity Assessment*, Contract No. 92−329 and 95−308; California Air Resources Board: Sacramento, CA, 2000.
(29) Lee, S.; Kim, H. K.; Yan, B.; Cobb, C. E.; Hennigan, C.; Nichols, S.; Chamber, M.; Edgerton, E. S.; Jansen, J. J.; Hu, Y.; Zheng, M.; Weber, R. J.; Russell, A. G. Diagnosis of aged prescribed burning plumes impacting an urban area. *Environ. Sci. Technol.* **2008**, *42*, 1438–1444.
(30) Hansen, D. A.; Edgerton, E. S.; Hartsell, B. E.; Jansen, J. J.; Kandasamy, N.; Hidy, G. M.; Blanchard, C. L. The Southeastern Aerosol Research and Characterization Study, part 3: Continuous measurements of fine particulate matter mass and composition. *J. Air Waste Manage. Assoc.* **2006**, *56* (9), 1325–1341.
(31) Sandberg, D. V.; Anderson, G. K.; Northeim, R. A. *Fire Emission Production Simulator Tutorial: Student Workbook*; USDA Forest Service: Washington, DC, 2005.
(32) Stauffer, D. R.; Seaman, N. L. Multiscale four-dimensional data assimilation. *J. Appl. Meteorol.* **1994**, *33*, 416–434.
(33) Alessio, G. A.; DeLillis, M.; Fanelli, M.; Pinelli, P.; Loreto, F. Direct and indirect impacts of fire on isoprenoid emissions from Mediterranean vegetation. *Funct. Ecol.* **2004**, *18*, 357–364.
(34) Puxbaum, H.; Tenze-Kunit, M. Size distribution and seasonal variation of atmospheric cellulose. *Atmos. Environ.* **2003**, *37*, 3693–3699.
(35) Turpin, B. J.; Lim, H.-J. Species contributions to $PM_{2.5}$ mass concentrations: Revisiting common assumptions for estimating organic mass. *Aerosol Sci. Technol.* **2001**, *35*, 602–610.
(36) Baumann, K.; Ift, F.; Zhao, J. Z.; Chameides, W. L. Discrete measurements of reactive gases and fine particle mass and composition during the 1999 Atlanta Supersite Experiment *J. Geophys. Res.* **2003***108*D78416, DOI: 10.1029/2001JD001210.
(37) Claeys, M.; Graham, B.; Vas, G.; Wang, W.; Vermeylen, R.; Pashynska, V.; Cafmeyer, J.; Guyon, P.; Andreae, M. O.; Artaxo, P.; Maenhaut, W. Formation of secondary organic aerosols through photooxidation of isoprene. *Science* **2004**, *303*, 1173–1176.
(38) Kavouras, I. G.; Mihalopoulos, N.; Stephanou, E. G. Formation of atmospheric particles from organic acids produced by forests. *Nature* **1998**, *395*, 683–686.
(39) Yan, B.; Zheng, M.; Hu, Y.; Lee, S.; Kim, H. K.; Russell, A. G. Organic composition of carbonaceous aerosols in an aged prescribed fire plume. *Atmos. Chem. Phys. Discuss.* **2007**, *7*, 18015–18042.
(40) Pun, B. K.; Seigneur, C. Investigative modeling of new pathways for secondary organic aerosol formation. *Atmos. Chem. Phys. Discuss.* **2007**, *7*, 2199–2216.
(41) Seigneur, C.; Moran, M. Chapter 8: Chemical transport models. In *Particulate Matter Science for Policy Makers: A NARSTO Assessment*; McMurry, P. H., Shepherd, M., Vickery, J., Eds.; Cambridge University Press, Cambridge, United Kingdom, 2004; pp 283−323.
(42) Morris, R. E.; Koo, B.; Guenther, A.; Yarwood, G.; McNally, D.; Tesche, T. W.; Tonnesen, G.; Boylan, J.; Brewer, P. Model sensitivity evaluation for organic carbon using two multi-pollutant air quality models that simulate regional haze in the southeastern United States. *Atmos. Environ.* **2006**, *40*, 4960–4972.
(43) Volkamer, R.; Jimenez, J. L.; Martini, F. S.; Dzepina, K.; Zhang, Q.; Salcedo, D.; Molina, L. T.; Worsnop, D. R.; Molina, M. J. Secondary organic aerosol formation from anthropogenic air pollution: Rapid and higher than expected *Geophys. Res. Lett.* **2006***33*L17811, DOI: 10.1029/2006GL026899.
(44) Liggio, J.; Li, S.-M.; Brook, J. R.; Mihele, C. Direct polymerization of isoprene and α-pinene in acidic aerosols. *Geophys. Res. Lett.* **2007**, *34*, L05814. doi:10.1029/2006GL028468.
(45) Gao, S.; NG, N. L.; Keywood, M.; Varutbangkul, V.; Bahreini, R.; Nenes, A.; He, J.; Yoo, K. Y.; Beauchamp, J. L.; Hodyss, R. P.; Flagan, R. C.; Seinfeld, J. H. Particle phase acidity and oligomer formation in secondary organic aerosol. *Environ. Sci. Technol.* **2004**, *38*, 6582–6589.
(46) Jang, M.; Czoschke, N. M.; Lee, S.; Kamens, R. M. Heterogeneous atmospheric aerosol production by acid-catalyzed particle-phase reactions. *Science* **2002**, (298), 814–817.
(47) Nopmongcol, U.; Khamwichit, W.; Fraser, M. P.; Allen, D. T. Estimates of heterogeneous formation of secondary organic aerosol during a wood smoke episode in Houston, Texas. *Atmos. Environ.* **2007**, *41*, 3057–3070.

ES071703K